Supporting information

NO reduction by carbon-based gases based on coal gasification fractions: NO reduction intermediate identification and kinetic analysis

Xiang Zhang [1], Jian Tian (✉)[1,2,3] , Tanghui Hu [1], Guangyong Yue [2,3], Xianlong Liu [2,3], Wen Zhou [3], Xiaohong Liu [3], Xinye Wang (✉)[4]

1 Ministry-of-Education Key Laboratory for the Green Preparation and Application of Functional Materials, Hubei Engineering Research Center for Green Industrialization Technology of Industrial Waste, School of Materials Science and Engineering, Hubei University, Wuhan 430062, China

2 Hubei Huda Tianshu New Energy Materials Industrial Research and Design Institute Co., Ltd., Wuhan 430062, China

3 Wuhan Tianshu Dust Removal Equipment Co., Ltd., Wuhan 430062, China

4 Engineering Laboratory for Energy System Process Conversion & Emission Control Technology of Jiangsu Province, School of Energy and Mechanical Engineering, Nanjing Normal University, Nanjing 210042, China

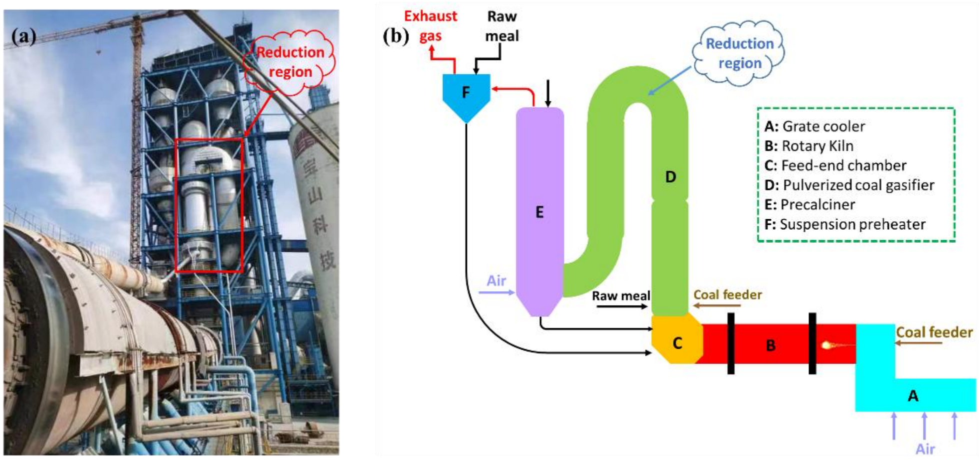

Fig. S1 Equipment and schematic diagram of denitration process of cement kiln coupled with pulverized coal gasifier. (a) Equipment diagram; (b) Schematic diagram.

✉ Corresponding authors
E-mail: tj-lily@sohu.com (J. Tian); xinye.wang@njnu.edu.cn (X. Wang)

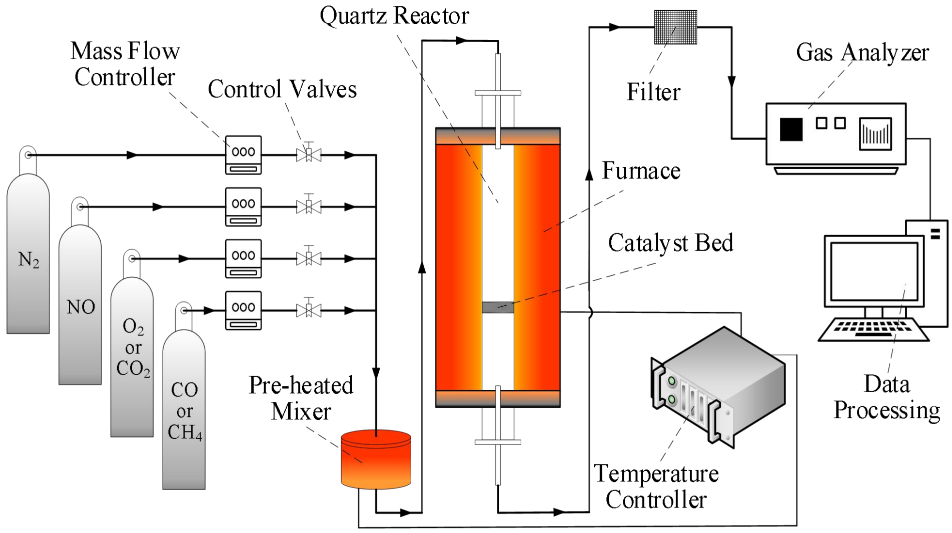

Fig. S2 Diagram of fixed bed reactor installation.

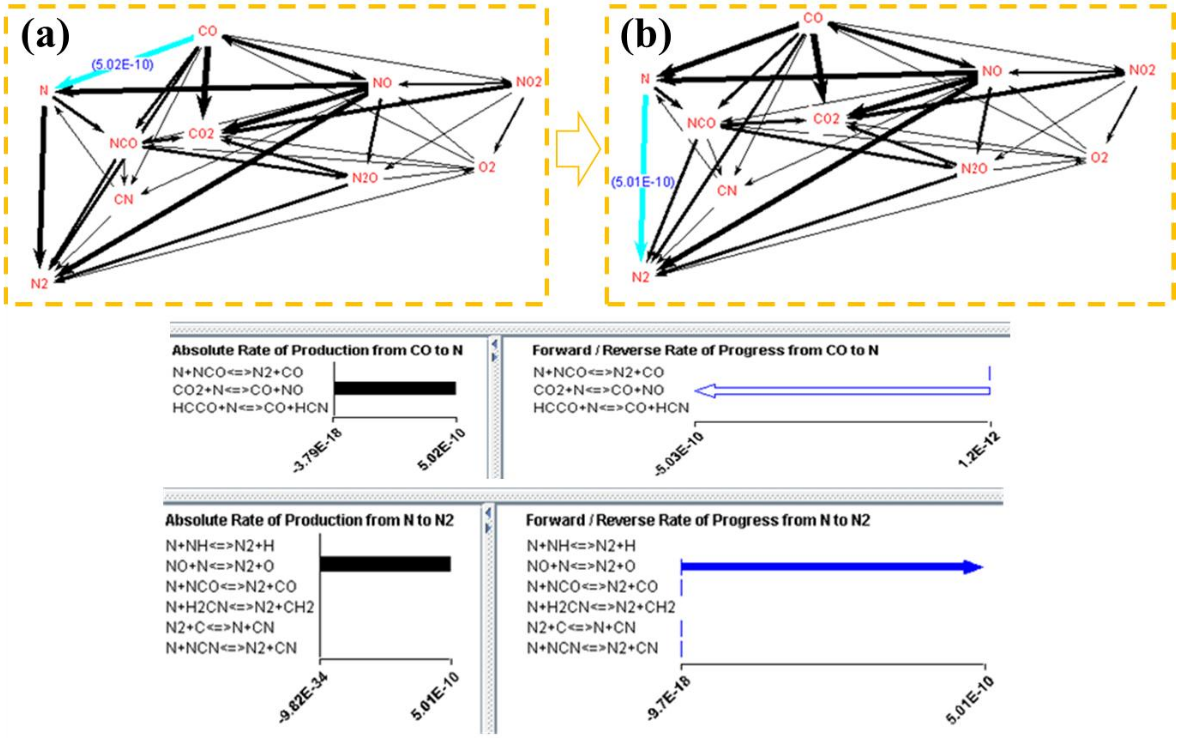

Fig. S3 Reaction pathway for conversion of NO to N_2 via N·. (a) NO to N·; (b) N· to N_2.

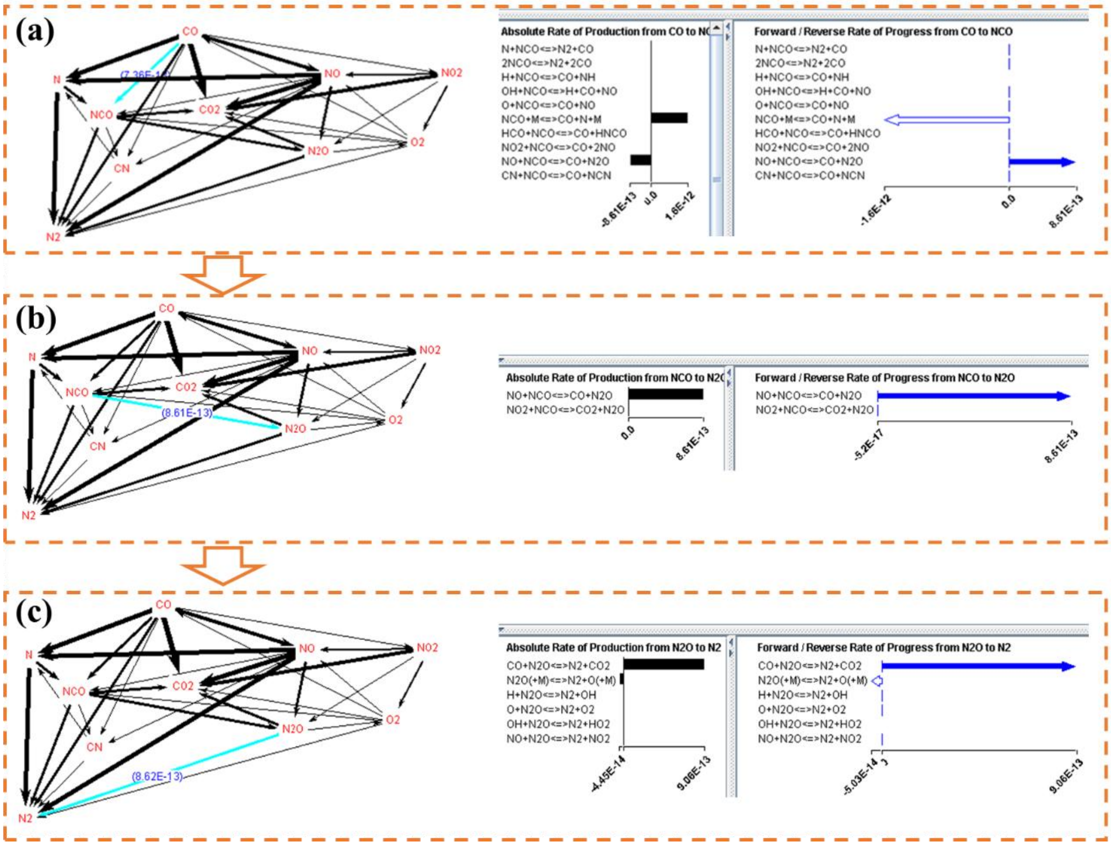

Fig. S4 Reaction pathway for conversion of NO to N_2 via NCO· and N_2O. (a) CO to NCO·; (b) NCO· to N_2O; (c) N_2O to N_2.

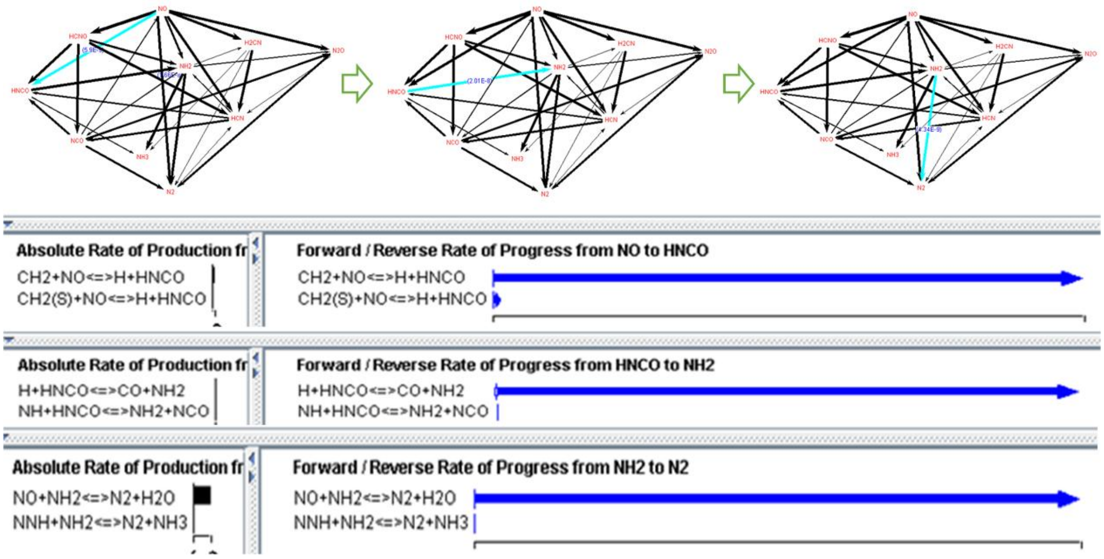

Fig. S5 Reaction pathway for conversion of NO to N_2 via HCNO· and NH_2·.

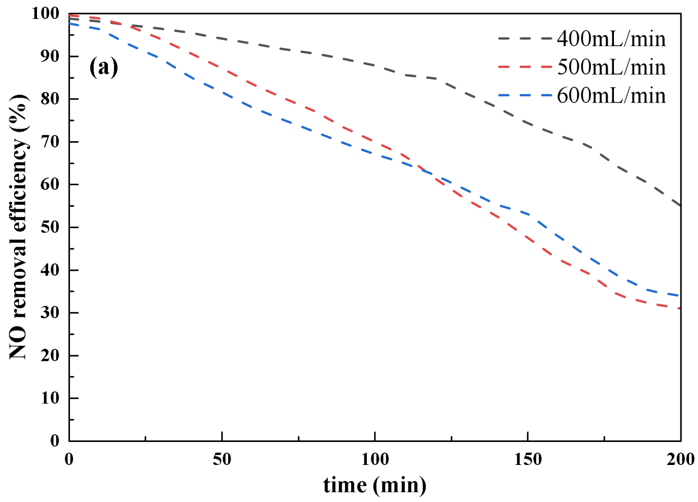

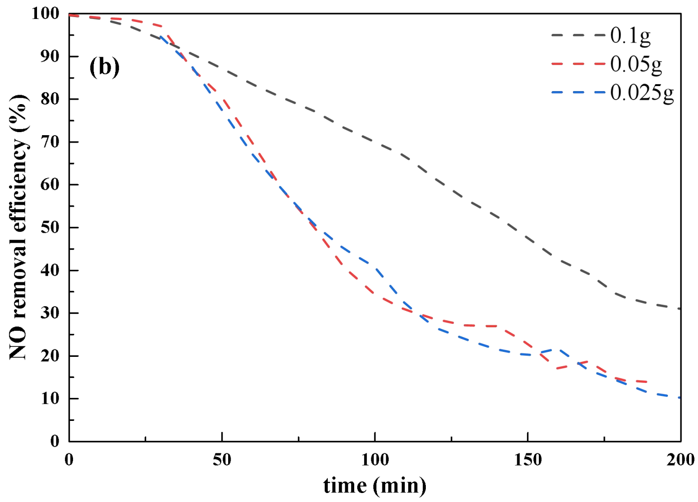

Fig. S6 Effect of gas flow and catalyst mass on denitration reaction rate. (a) effect of gas flow; (b) effect of catalyst mass.

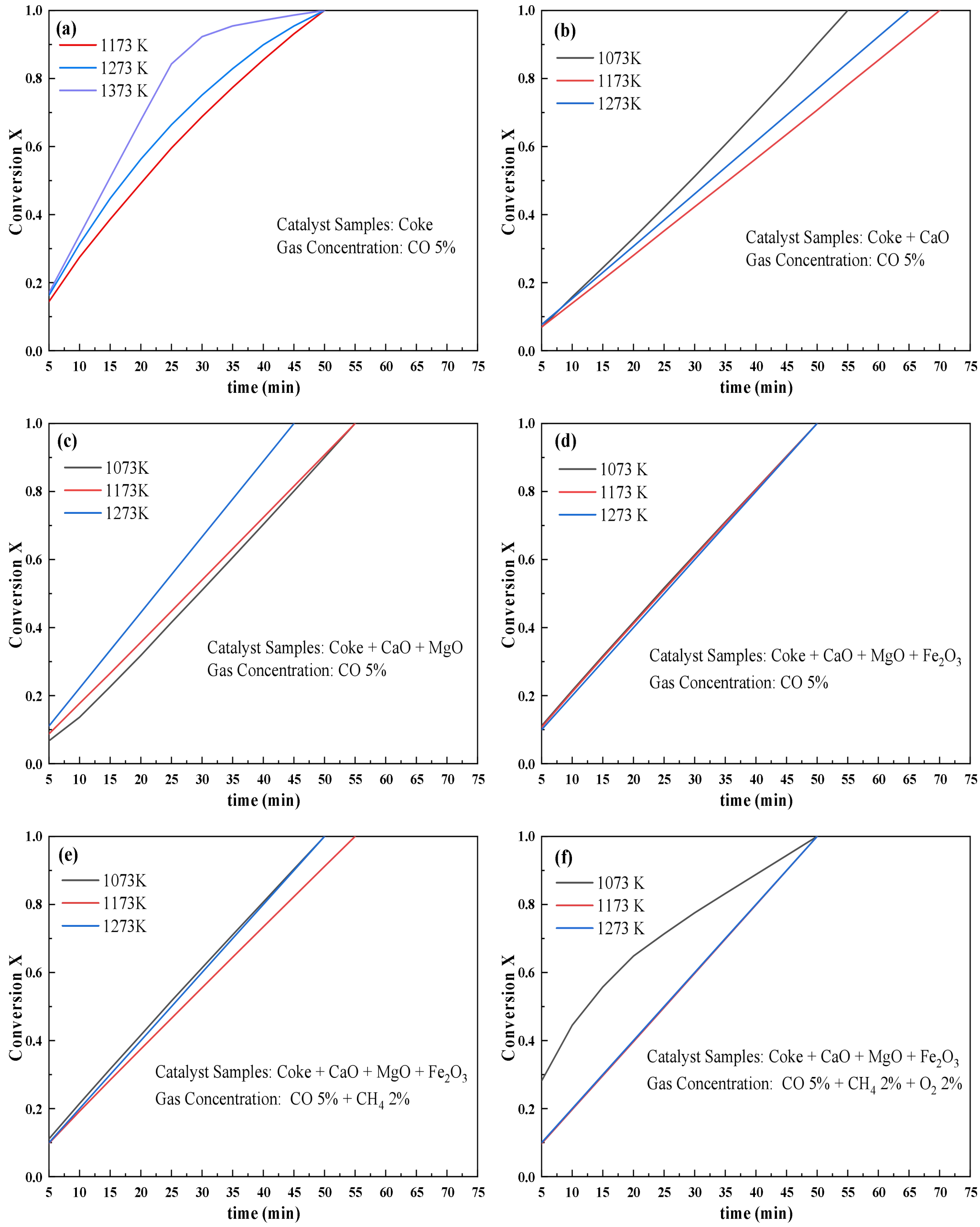

Fig. S7 NO conversion rate as a function of time. (a) Coke (CO 5%); (b) Coke + CaO (CO 5%); (c) Coke + CaO + MgO (CO 5%); (d) Coke + CaO + MgO + Fe_2O_3 (CO 5%); (e) Coke + CaO + MgO + Fe_2O_3 (CO 5% + CH_4 2%); (f) Coke + CaO + MgO + Fe_2O_3 (CO 5% + CH_4 2% + O_2 2%).

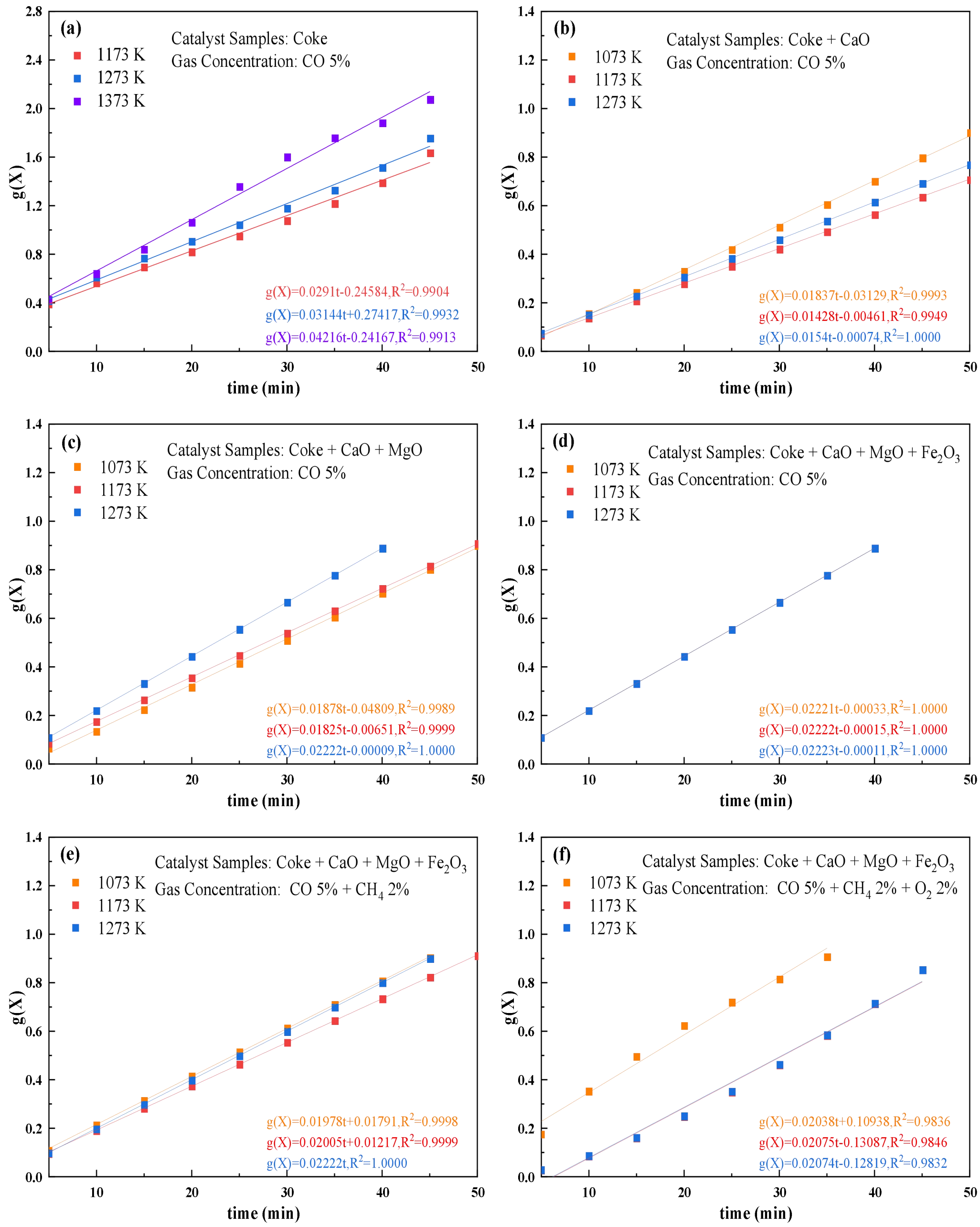

Fig. S8 Fitting test based on reaction kinetic model. (a) Coke (CO 5%); (b) Coke + CaO (CO 5%); (c) Coke + CaO + MgO (CO 5%); (d) Coke + CaO + MgO + Fe_2O_3 (CO 5%); (e) Coke + CaO + MgO + Fe_2O_3 (CO 5% + CH_4 2%); (f) Coke + CaO + MgO + Fe_2O_3 (CO 5% + CH_4 2% + O_2 2%).

Table S1 Flue gas fraction at the end of rotary kiln.

Components*	Content
CO_2 %	15.0
O_2 %	2.1
N_2 %	82.9
NO ppm	1077.3
NO_2 ppm	119.7

Notes: * Dry based

Table S2 The parameters of the PFR model.

Parameters	Value
Temperature (K)	1073–1773
NO %	0.1197
CO %	0.5–20
CH_4 %	2–8
H_2 %	1–10
CO_2 %	2–5
O_2 %	1–5
H_2O %	2–5
N_2 %	Balance gas

Table S3 Experimental conditions of denitration kinetics.

Samples	Weight (g)	Temperature (K)	Total gas flow (mL/min)	NO concentration (ppm)	Gas concentration (%)
Coke	0.025	1073–1373	500	1200	CO 5%
Coke + CaO	0.025	1073–1373	500	1200	CO 5%
Coke + CaO + MgO	0.025	1073–1373	500	1200	CO 5%
Coke + CaO + MgO + Fe_2O_3	0.025	1073–1373	500	1200	CO 5%
Coke + CaO + MgO + Fe_2O_3	0.025	1073–1373	500	1200	CO 5% + CH_4 2%
Coke + CaO + MgO + Fe_2O_3	0.025	1073–1373	500	1200	CO 5% + CH_4 2% + O_2 2%

Table S4 Kinetic mechanism model and description.

No.	Kinetic Model		$f(X)$	$g(X)$
1	power law		$4X^{3/4}$	$X^{1/4}$
2	power law		$3X^{2/3}$	$X^{1/3}$
3	power law		$2X^{1/2}$	$X^{1/2}$
4	power law		$2/3X^{-1/2}$	$X^{3/2}$
5	contraction model	zero order	1	X
6	contraction model	2-D	$2(1-X)^{1/2}$	$1-(1-X)^{1/2}$
7	contraction model	3-D	$3(1-X)^{2/3}$	$1-(1-X)^{1/3}$
8	kinetics-order models	first order	$(1-X)$	$-\ln(1-X)$
9	kinetics-order models	3/2 order	$(1-X)^{3/2}$	$2[(1-X)^{-1/2} - 1]$
10	kinetics-order models	second order	$(1-X)^2$	$(1-X)^{-1} - 1$
11	kinetics-order models	third order	$(1-X)^3$	$1/2[(1-X)^{-2} - 1]$
12	nucleation model	$n = 1.5$	$3/2(1-X)[-\ln(1-X)]^{1/3}$	$[-\ln(1-X)]^{2/3}$
13	nucleation model	$n = 2$	$2(1-X)[-\ln(1-X)]^{1/2}$	$[-\ln(1-X)]^{1/2}$
14	nucleation model	$n = 3$	$3(1-X)[-\ln(1-X)]^{2/3}$	$[-\ln(1-X)]^{1/3}$
15	nucleation model	$n = 4$	$4(1-X)[-\ln(1-X)]^{3/4}$	$[-\ln(1-X)]^{1/4}$
16	diffusion model	1-D	$1/(2X)$	X^2
17	diffusion model	2-D	$1/[-\ln(1-X)]$	$(1-X)\ln(1-X) + X$
18	diffusion model	3-D(Jander)	$(3/2)(1-X)^{2/3} [1-(1-X)^{1/3}]$	$[1-(1-X)^{1/3}]^2$
19	diffusion model	3-D(Grinstling)	$(3/2)[(1-X)^{-1/3} - 1]$	$(1-2X/3)-(1-X)^{2/3}$

Table S5 Relevant elementary reaction and kinetic parameters.

No.	Reaction	*A*	E_a
R1	$CO + NO \leftrightarrow CO_2 + N\cdot$	1.17E + 16	48038
R2	$NO + N\cdot \leftrightarrow N_2 + O\cdot$	3.30E + 12	0
R3	$NO + NCO\cdot \leftrightarrow N_2O + CO$	1.900E + 17	740
R4	$NO + NCO\cdot \leftrightarrow N_2 + CO_2$	3.800E + 18	800
R5	$CO + N_2O \leftrightarrow CO_2 + N_2$	3.20E + 11	20237
R6	$CH_2 + NO \leftrightarrow H\cdot + HCNO\cdot$	3.1E + 17	1270
R7	$HCNO\cdot + H\cdot \leftrightarrow CO + NH_2\cdot$	2.25E + 07	15844
R8	$NH_2\cdot + NO \leftrightarrow N_2 + H_2O$	1.30E + 16	0
R9	$HCNO\cdot + O\cdot \leftrightarrow NCO\cdot + OH\cdot$	2.20E + 06	47652
R10	$HCNO\cdot + OH\cdot \leftrightarrow NCO\cdot + H_2O$	3.30E + 07	15048
R11	$CH_3\cdot + NO \leftrightarrow H_2CN\cdot + OH\cdot$	1.00E + 12	90915
R12	$HCN\cdot + O\cdot \leftrightarrow NCO\cdot + H\cdot$	2.03E + 04	20816
R13	$N_2O\cdot + H\cdot \leftrightarrow N_2 + OH\cdot$	3.87E + 14	78918